HHS Public Access

Author manuscript

Cancer Res. Author manuscript; available in PMC 2016 November 15.

Published in final edited form as:

Cancer Res. 2015 November 15; 75(22): 4910–4922. doi:10.1158/0008-5472.CAN-15-0797.

Heightening energetic stress selectively targets LKB1-deficient non-small cell lung cancers

Milica Momcilovic[1], **Robert McMickle**[1], **Evan Abt**[3], **Atsuko Seki**[2], **Sarah A. Simko**[1], **Clara Magyar**[2], **David B. Stout**[3], **Michael C. Fishbein**[2], **Tonya C. Walser**[1], **Steven M. Dubinett**[1], and **David B. Shackelford**[1,*]

[1]Department of Pulmonary and Critical Care Medicine, David Geffen School of Medicine, University of California, Los Angeles, CA 90095

[2]Department of Pathology and Laboratory Medicine, David Geffen School of Medicine, University of California, Los Angeles, CA 90095

[3]Department of Pharmacology, David Geffen School of Medicine, University of California, Los Angeles, CA 90095

Abstract

Inactivation of the LKB1 tumor suppressor is a frequent event in non-small cell lung carcinoma (NSCLC) leading to the activation of mammalian target of rapamycin complex 1 (mTORC1) and sensitivity to the metabolic stress inducer phenformin. In this study, we explored the combinatorial use of phenformin with the mTOR catalytic kinase inhibitor MLN0128 as a treatment strategy for NSCLC bearing co-mutations in the *LKB1* and *KRAS* genes. NSCLC is a genetically and pathologically heterogeneous disease, giving rise to lung tumors of varying histologies that include adenocarcinomas (ADCs) and squamous cell carcinomas (SCCs). We demonstrate that phenformin in combination with MLN0128 induced a significant therapeutic response in *KRAS/LKB1* mutant human cell lines and genetically engineered mouse models of NSCLC that develop both ADCs and SCCs. Specifically, we found that *KRAS/LKB1* mutant lung ADCs responded strongly to phenformin + MLN0128 treatment, but the response of SCCs to single or combined treatment with MLN0128 was more attenuated due to acquired resistance to mTOR inhibition through modulation of the AKT-GSK signaling axis. Combinatorial use of the mTOR inhibitor and AKT inhibitor MK2206 robustly inhibited the growth and viability of squamous lung tumors thus providing an effective strategy to overcome resistance. Taken together, our findings define new personalized therapeutic strategies that may be rapidly translated into clinical use for the treatment of *KRAS/LKB1* mutant adenocarcinomas and squamous cell tumors.

* corresponding author.

The authors declare there are no conflicts of interest.

Author contributions: M.M., R.J.M., and E.A. performed all cell experiments with assistance from S.A.S. M.M. performed all mouse experiments with assistance of R.M. and E.A. M.M., R.J.M., and E.A., analyzed the data. D.B.S. designed the study and wrote the paper. M.C.F and A.S. are board-certified anatomic pathologists who performed all pathological analysis. C.M. performed all Definiens analysis. T.C.W. and S.M.D. contributed resources and critical feedback on the project. D.S. reviewed PET and CT scans on the mice.

Competing interests: The authors declare that they have no competing interests.

Keywords

LKB1; phenformin; NSCLC; mTOR; FDG-PET

Introduction

Currently, there are few effective, targeted therapies for the treatment of non-small cell lung cancer (NSCLC) and no effective strategies for the chemoprevention of lung cancer. Successful targeted therapies for NSCLC, including inhibitors against *EGFR* and *ALK* mutant tumors, treat only a subset adenocarcinoma (ADC) patients(1,2), leaving the vast majority of patients with ADC and squamous cell carcinoma (SCC) without targeted therapeutic options(3). The *LKB1* tumor suppressor is a master regulator of cellular growth, metabolism and survival that is inactivated in up to 20-30% of NSCLC(4-6). In a recent study we demonstrated that the biguanide phenformin, a mitochondrial complex I inhibitor and metabolic stress inducer selectively induced apoptosis in LKB1-deficient (LKB1−/−) NSCLC cells(7). Phenformin induced a significant therapeutic response in $Kras^{G12D}$ driven, *Lkb1*−/− (*Kras/Lkb1*) genetically engineered mouse models (GEMMs) of NSCLC leading to increased tumor cell apoptosis, slowing tumor progression and extending overall survival. However, phenformin was not curative as a single agent, underscoring the need to identify additional pathways to combinatorially target.

Loss of LKB1 leads to hyper-activation of mTORC1 signaling in a cell autonomous manner thus making mTORC1 an attractive target to inhibit in LKB1-deficient lung tumors(8). Elevated mTORC1 activation results in increased expression of targets, such as hypoxia inducible factor 1 alpha and 2 alpha (HIF1α and HIF2α), which actively drive cell growth and a glycolytic metabolic signature seen in a variety of human tumors(9-11). In previous work we successfully inhibited polyp formation and glucose metabolism in a *Lkb1*+/− model of Peutz Jeghers Syndrome using the allosteric mTORC1 inhibitor rapamycin suggesting that inhibition of mTORC1 is a viable strategy to target LKB1−/− NSCLC(10). However, rapamycin as a single agent failed to induce a therapeutic response in the *Kras/Lkb1* mouse model of lung cancer and rapalogs have demonstrated limited benefit for NSCLC in the clinic(12,13). These data suggested the need to evaluate next generation mTOR catalytic kinase inhibitors to target LKB1-deficient lung tumors. MLN0128 is a potent mTOR catalytic kinase inhibitor that has shown efficacy as an anti-cancer agent in cell culture and xenograft models of sarcoma, neuroblastoma and pancreatic cancer(14), (15,16) as well as GEMMs of *Pten*−/− prostate cancer and *Myc* driven lymphoma(17,18). MLN0128 is currently in clinical trials for treatment of advanced solid tumors and hematological malignancies (NCT01351350; NCT01118689). In this study we explored the combinatorial use of phenformin with MLN0128 as a therapeutic strategy to target *KRAS/LKB1* mutant lung tumors.

Methods

Cell culture

Cells were maintained at 37°C in a humidified incubator with 5% CO_2. A549, H460, A427, H838, H23, H157, H596, H1703, H226 and SW900 cells were obtained from ATCC. H1568, H441, and RH2 lung cancer cell lines were a kind gift from Dr. Steven Dubinett (UCLA). All cell lines were routinely tested and confirmed to be free of Mycoplasma using the MycoAlert Mycoplasma Detection Kit (Lonza Walkersville). Cell lines were authenticated in the UCLA Genotyping and Sequencing Core utilizing Promega's DNA IQ System and Powerplex 1.2 system, and all cells were utilized within 10 passages of genotyping. Cells were grown in Dulbecco's modified Eagle's medium (DMEM) or RPMI 1640 medium (Corning) plus 5% fetal bovine serum (Hyclone, Logan, UT, USA) and 1% penicillin/streptomycin (Gibco).

NOVA metabolite measurement

Media was collected from tissue culture plates and analyzed for glucose and lactate concentrations using the Bioanalyzer 4 (Nova Biomedical). Cells were seeded into 6cm plates overnight and were subsequently treated with 2μM MLN0128 or DMSO in fresh DMEM medium (Corning) for 24 hours. Metabolite concentrations were normalized to cell number.

Antibodies and reagents

For *in vitro* studies MLN0128 (Selleckchem Houston, TX, USA) was dissolved in DMSO, phenfomin was dissolved in DMEM. For *in vivo* studies MLN0128 was dissolved in 1-methyl-2-pyrrolidinone (NMP), then diluted in 15% PEG diluted in water; phenformin was diluted in water at 1.8 mg/ml. Rapamycin was purchased from LC Laboratories (Woburn, MA) and dissolved in DMSO. Antibodies from Cell Signaling Technology (Beverly, MA, USA) used for immunoblots were diluted 1:1,000 and included phospho-p70 S6 kinase (Thr389 #9234), phospho-S6 (Ser235/236 #4858), total 4E-BP1 (#9644), phospho-4E-BP1 (Thr37/46 #2855), phospho-Akt (Ser473 #4060), phospho-Akt (Thr308 #4056), phospho-NDRG1 (Thr346 #5482), Phospho-Tuberin/TSC2 (Thr1462 #3611), phospho-GSKα/β (Ser21/9 #9331), beta-actin (#4970), cleaved PARP (Asp214 #5625), cleaved caspase 3 (Asp175 #9661) and phospho-Raptor (Ser792 #2083). Anti-Hif-1alpha (C-Term #10006421 1:200) antibody was purchased from Cayman Chemical and anti-GLUT1 (GT11-A 1:1,000) antibody was purchased from Alpha Diagnostic International (San Antonio, TX, USA). Plasmid expressing dox-inducible *4EBP1 4Ala* (pCW57.1-4EBP1_4xAla, plasmid # 38240) and control vector (pCW57.1, plasmid # 41393) were purchased from Addgene.

Therapeutic studies in mice

We performed pharmacodynamics (PD) studies testing the combinatorial delivery of phenformin + MLN128 in wildtype FVB mice. We treated mice for three weeks with either vehicle, MLN0128 (1.0mg/kg/q.d.) by i.p. injection, phenformin (in water 1.8mg/mL/ad lib) or the combination of phenformin + MLN128 for 6 days on and 1 day off. Due to the lengthy 8-week treatment regimen outlined in our pre-clinical studies, we opted for once

daily i.p. injection of MLN0128 and ad lib delivery of phenformin to reduce the stress of daily treatments on mice. This proved beneficial as our mice showed no adverse weight loss or morbidity to treatment regimens (unpublished data). At the end of three weeks treatment mice were euthanized and lung tissue was collected for biomarker analysis by immunoblot.

We performed therapeutic studies using Lox-Stop-Lox Kras G12D, Lkb1 Lox/Lox, Rosa26-Lox-Stop-Lox-Luc mice (KL_{luc}) and Lox-Stop-Lox Kras G12D, Rosa26-Lox-Stop-Lox-Luc mice (K_{luc}) that were obtained from Reuben Shaw at Salk Institute for Biological Studies[7]. All mice were on a FVB background. Lung tumors were induced by intranasal administration of 2.5×10^6 plaque forming units of Adeno-Cre (Gene Transfer Vector Core, University of Iowa) as previously described[7]. For therapeutic studies KL_{luc} and K_{luc} mice were randomly sorted into four groups: vehicle, phenformin, MLN0128 and phenformin +MLN0128. Treatment with indicated drugs was initiated 4 weeks post Adeno-Cre delivery for KL_{luc} mice or 8 weeks post Adeno-Cre delivery for K_{luc} mice. Phenformin was delivered adlib at 1.8 mg/ml in the drinking water and changed weekly. MLN0128 was delivered in NMP/15% PEG i.p at 1mg/kg once a day. Vehicle group received NMP/15% PEG i.p. once a day. Both MLN0128 and vehicle were prepared daily. Mice were housed in pathogen-free facilities at University of California Los Angeles (UCLA). All experimental procedures performed on mice were approved by the UCLA Animal Research Committee.

Histology and immunohistochemical analysis

Tissue isolation, fixation and staining procedures were performed as previously described in Shackelford et al., 2013. Briefly, the following antibodies were used: phospho-4E-BP1 (Thr37/46) (Cell Signaling Technology, #2855 1:1600), cleaved caspase-3 (Asp175) (Cell Signaling Technology, #9661 1:200), anti-p63 (4A4) (abcam, #ab111449 1:100), anti-TTF-1 (8G7G3/1) (Dako, 1:200), anti-Ki67 (SP6) (Thermo Scientific, #RM-9106-S0 1:200), phospho-S6 (Cell Signaling Technology, #4585 1:400), hexokinase II (Cell Signaling Technology, #2867 1:800), phospho-AMPKα (Thr172) (40H9) (Cell Signaling Technology, #2535 1:100), phospho-p44/42 MAPK (Erk1/2) (Thr202/Tyr204) (D13.14.4E) XP (Cell Signaling Technology, #4370 1:400), phospho-GSKα/β (Ser21/9) (Cell Signaling Technology, #9331 1:50). Immunostained slides were digitally scanned onto a ScanScope AT (Aperio Technologies, Inc., Vista, CA). A pathologist blindly evaluated the H&E stained sections for distribution of histological subtypes, verified by p63 and TTF-1 immunostaining, and calculated the percentage of positively stained cells for Ki67, cleaved caspase-3, phospho-S6, and hexokinase II. Digital slides were analyzed with the Definiens' Tissue Studio (Definiens Inc. Parsippany, NJ) to determine adenocarcinoma tumor area and necrotic tumor area.

Microplate and flow cytometry analysis

These assays were performed as previously described Shackelford, et al., 2013.

Results

Phenformin and MLN0128 combination therapy compound energy stress and induce apoptosis in *LKB1* mutant NSCLC cells

In a previous study we identified the mTORC1 substrate phospho-4E-BP1 (P-4E-BP1) remained highly upregulated in *Kras*^{G12D};*Lkb1*−/−;*Luc* (KL$_{luc}$) mouse lung tumors following phenformin treatment(7). We hypothesized sustained mTORC1 activation may contribute to phenformin resistance and this provided the rationale to inhibit mTORC1 in combination with phenformin. We performed a dose escalation analysis of the allosteric mTORC1 inhibitor rapamycin or the mTOR kinase inhibitor MLN0128 on the *KRAS/LKB1* mutant NSCLC cell line A549 and showed that low dose MLN0128 potently inhibited mTORC1 through phospho-S6K (P-S6K), phospho-S6 (P-S6) and phospho-4E-BP1 (P-4E-BP1) as well as mTORC2 through inhibition of phospho-AKTthr473 (P-AKT473) and phospho-NDRG1 (P-NDRG1) (**Figure 1A**)(19). Rapamycin failed to inhibit mTORC2 and partially suppressed mTORC1 signaling through inhibition of P-S6K but not P-4E-BP1 (**Figure 1A**)(20). We next performed a high throughput analysis of phenformin alone or in combination with MLN0128 on a panel of *LKB1* mutant (*LKB1*−/−) NSCLC cell lines that were both positive and negative for *KRAS* mutations. *LKB1*−/−, *KRAS* wildtype lines include: H838, and H1568, while *KRAS/LKB1* mutant tumor lines included: A549, H460, H157, RH2, A427, and H23. We measured both cellular ATP and apoptosis using the cell titer glo or cleaved caspase 3/7 glo assays, respectively as a readout of apoptosis following a 24 hour treatment of cells with either vehicle, phenformin, MLN0128 or phenformin + MLN0128. We found that phenformin + MLN0128 treatment significantly reduced cellular ATP and induced higher levels of apoptosis compared to either single therapy alone or vehicle controls (**Figure 1B, C**). Additionally, we found that phenformin + MLN0128 did not significantly reduce cellular ATP levels in *KRAS* mutant *LKB1* wildtype human NSCLC cell lines compared to phenformin single therapy (**Figure S1A**). We next examined whether rapamycin (RAPA) induced energetic stress in panels of *LKB1* wildtype and *LKB1* mutant NSCLC cell lines and detected no change in cellular ATP levels between the untreated controls and RAPA treated cells (**Figure S1B**). These results demonstrated that MLN0128 but not RAPA was a potent inducer of energetic stress. For the duration of the study we focused on using only MLN0128 as a single agent or in combination with phenformin.

We next confirmed LKB1 inactivation dictated sensitivity to phenformin + MLN0128 combination therapy by screening *KRAS/LKB1* mutant A549 isogenic cell lines expressing pBABE vector (B), expressing functional LKB1 (WT) or kinase dead inactive LKB1 (KD). Following treatment with vehicle, phenformin, MLN0128 or phenformin + MLN0128, we measured apoptosis by staining for AnnexinV, cleaved caspase 3 or cleaved PARP and using flow cytometry and immunoblots, respectively. Cells expressing functional LKB1-WT showed a significant reduction in AnnexinV levels compared to cells expressing vector alone (pBABE) or kinase dead LKB1 (LKB1-KD) thus demonstrating LKB1 inactivation sensitized NSCLC cells to apoptosis following treatment with phenformin or phenformin + MLN0128 (**Figure 1D, S1C**). These results demonstrated that phenformin and MLN0128 cooperate to compound energy stress and enhance apoptosis in LKB1 mutant NSCLC tumor lines as compared to either therapy alone.

4E-BP1 is a critical regulator of cell survival and energetics in human *KRAS/LKB1* mutant NSCLC tumor cells

We first sought to examine whether 4E-BP1, a direct mTORC1 substrate was critical regulator of cell growth in survival in *KRAS/LKB1* mutant NSCLC tumors. Previous studies have shown that 4E-BP1 is a critical mediator of tumor cell proliferation and survival downstream of mTOR signaling in normal and cancer cells(21). We took advantage of a doxycycline (dox) inducible mutant 4E-BP1 *4Ala* (4E-BP1 4A) that constitutively binds eIF4E to inhibit cap dependent translation(22,23). We reasoned that the 4E-BP1 4A mutant would mimic MLN0128 mediated inhibition of *4E-BP1* and cooperate with phenformin to induce energy stress and apoptosis in *KRAS/LKB1* mutant NSCLC cells. *KRAS/LKB1* mutant A549 and H460 lines expressing 4E-BP1 4A (A549-4E-BP1 4A, H460-4E-BP1 4A) had a two fold reduction of cell growth after 72 hours of dox treatment (**Figure 2A**). Expression of dominant negative 4E-BP1 alone in *KRAS/LKB1* mutant cells did not inhibit glycolysis suggesting growth inhibition may be mediated by suppression of cap dependent translation (**Figure S2A**). Phenformin cooperated with expression of 4E-BP1 4A in H460 cell lines to induce a significant reduction in cell growth as compared to no treatment or single treatment controls (**Figure 2B**). Furthermore, 4E-BP1 4A expression in combination with phenformin enhanced apoptosis in H460-4E-BP1 4A cell lines (**Figure 2C**). Measurement of cellular ATP levels in H460-4E-BP1 4A cells treated with phenformin + dox showed a significant reduction in cellular ATP levels as compared to no treatment or single treatment controls (**Figure 2D**). Additionally, phenformin treatment of H460-4E-BP1 4A cells significantly reduced cellular ATP levels as compared to cells expressing vector alone (**Figure 2D**). These results demonstrate that inhibition of 4E-BP1 sensitized *KRAS/LKB1* mutant NSCLC tumor lines to energetic stress induced by phenformin.

MLN0128 is a potent *in vivo* mTORC1 inhibitor and suppressed glucose metabolism in *KRAS/LKB1* mutant NSCLC tumor lines

We sought to perform an *in vivo* evaluation of MLN0128 mediated mTOR inhibition in KL_{luc} lung tumors. Mice were treated with MLN0128 for five days at 1.0mg/kg/q.d. then lung nodules were isolated for biochemical and histological analysis. MLN0128 potently inhibited mTORC1 targets PS6K and P-4E-BP1 and mTORC2 target P-NDRG1 in KL_{luc} lung tumor nodules as shown by immunoblots and immunohistochemistry (**Figure 3A, B**). Interestingly, MLN0128 failed to inhibit phosphorylation of AKT at serine 473 suggesting a partial inhibition of mTORC2 *in vivo* (**Figure 3A)**. We next examined targets downstream of mTORC1 that included HIF1α and its targets GLUT1 – both critical regulators of glycolysis in *LKB1*−/− cells following MLN0128 treatment(10,24). *KRAS/LKB1* mutant H460 cells treated with MLN0128 for 24 or 48 hours showed durable inhibition of HIF1α and GLUT1 (**Figure 3C**). Next, we probed lung tumor lysates from KL_{luc} mice treated with 1.0mg/kg/q.d. MLN0128 for 5 days and discovered MLN0128 induced inhibition of Hif1α and Glut1 as well as a robust inhibition of hexokinase II (HkII) (**Figure 3D**). Examination of glycolysis in *KRAS/LKB1* mutant human and mouse NSCLC tumor lines treated with MLN0128 for 24 hours significantly reduced glucose consumption and lactate production (**Figure 3E, F**). We then performed biomarker analysis on normal lung tissue lysates from wildtype FVB mice that were administered vehicle, phenformin (1.8mg/mL ad lib),

MLN0128 (1.0mg/kg/q.d.) or phenformin + MLN0128 for three weeks. Lysates were probed for P-4E-BP1, P-Akt S473 and P-Ndrg1 to measure mTORC1/C2 inhibition and P-Ampk as a marker of phenformin induced metabolic stress(7,25). Phenformin alone or in combination with MLN0128 activated P-Ampk while MLN0128 single or combination therapy inhibited P-4E-BP1, P-Akt S473 and P-Ndrg1 (**Figure S3A**). These results show MLN0128 is a potent inhibitor of mTOR signaling and key regulators of glycolysis *in vivo* as well as a suppressor of glucose metabolism in NSCLC tumor cell lines.

18F-FDG PET/CT guided studies in KL_{luc} mice revealed phenformin and MLN0128 treatment induced both a metabolic and therapeutic response in lung tumors

We then performed an FDG PET/CT guided preclinical studies in KL_{luc} mice as previously described (7) to evaluate efficacy of phenformin in combination with MLN0128 to target $Kras^{G12D}$ driven, *Lkb1−/−* lung tumors *in vivo*. Our use of FDG PET/CT imaging of mice were to measure therapeutic response as well as detect therapy resistant nodules in mice in real time. The treatment regimen and imaging analysis is outlined in **Figure 4A**. Analysis of tumor volume by CT scans and FDG uptake by PET imaging demonstrated significant suppression of tumor growth and glucose avidity after 6 weeks of treatment in single or combination therapy compared to vehicle (**Figures 4B-D right panels**). However, FDG PET and CT imaging detected distinct lung tumor nodules that rapidly developed by week 8 of treatment indicating tumors had developed resistance to phenformin and MLN0128 single and combination therapy (**Figure 4B-D left panels**). Interestingly, SUVmax measurements of lung tumor nodules at 8 weeks of treatment revealed that MLN0128 significantly reduced FDG avidity the entire 8 week course of treatment while cohorts treated with phenformin alone or in combination with MLN0128 developed FDG avid tumors by week 8 of treatment (**Figure 4D left panel**).

We next tested phenformin and MLN0128 as single agents or in combination on K_{luc} mice, which develop lung tumors with functional *Lkb1*(7). Due to the longer 15-20 week latency of lung tumor development in the K_{luc} model, as compared to 10-12 weeks in the KL_{luc} mice, we began a treatment regimen in K_{luc} mice at 50 days post lung tumor induction. FDG PET and CT imaging analysis of K_{luc} mice treated with phenformin and/or MLN0128 showed neither drug alone or in combination significantly suppressed tumor burden or FDG uptake after 8 weeks of treatment (**supplemental Figure S4A-C**). Results from CT scans suggest K_{luc} and KL_{luc} lung tumors may bypass mTOR inhibition and phenformin induced energetic stress to acquire therapy resistance. Interestingly, FDG PET imaging of mice showed that MLN0128 suppressed glucose uptake and tumor growth most significantly in KL_{luc} as compared to K_{luc} lung tumors confirming that metabolic sensitivity to MLN0128 was dependent upon *Lkb1* inactivation.

KL_{luc} adeno and squamous lung tumors differentially respond to MLN0128 therapy alone or in combination with phenformin

Histological analysis of hematoxylin and eosin (H&E) stained lung tumors showed that phenformin and MLN0128 as single or combined therapy significantly reduced the tumor burden (**Figure 5A**). The distinct nodules that were consistently present in the lungs of MLN0128 and phenformin + MLN0128 cohorts as detected by PET/CT imaging in Figure 4

prompted us to perform detailed histological analysis of therapy responsive and resistant tumors. Due to the complex heterogeneity of lung tumor subtypes in KL_{luc} mice – that include both ADC and SCC, we performed a detailed examination of the lung tumor subtypes distribution(26). We identified a higher prevalence of lung SCC in mice treated with phenformin (4/7 mice), MLN0128 (5/7 mice) or combination therapy (6/7) than vehicle treated mice (2/7 mice) (**Figure 5B**). We also observed a decrease in the total distribution of ADC in phenformin, MLN0128 and combination therapy cohorts compared to vehicle treated mice (**Figure 5B**). There was a significant increase in percentage of SCC tumors in the phenformin + MLN0128 treatment group compared to vehicle ($p < 0.05$). Conversely, there was also a significant decrease in the percentage of ADC tumors in the phenformin + MLN0128 treatment group as compared to vehicle ($p < 0.01$). The differences in distributions of SCC and ADC tumor subtypes for single treatments were not statistically significant as compared to vehicle or combination therapy. Immunohistochemical staining of lung tumors confirmed that the larger therapy resistant lung tumors were in fact p63 positive, TTF1 negative SCC while the smaller residual lesions were ADC (**Figure 5C**). We measured total tumor area of ADCs in H&E stained lung sections represented in Figure 5A using morphometric Definiens software. Analysis showed phenformin + MLN0128 combination therapy significantly reduced tumor burden and total lesions in lung ADC greater than either therapy alone or the vehicle controls suggesting that this treatment regimen is cytotoxic to ADC cells (**Figure 5D and 5E**). In contrast, a modest but insignificant decrease in tumor burden and total lesion were observed in K_{luc} mice that received therapy as compared to the vehicle group (**supplemental Figure S5A-C**). Taken together these results demonstrate that KL_{luc} mutant lung ADCs are uniquely sensitive to MLN0128 and phenformin + MLN0128 therapy while SCC acquired resistance late in treatment.

Phenformin and MLN0128 combination therapy enhanced tumor cell apoptosis while suppressing proliferation, mTORC1 and Hexokinase II expression in KL_{luc} lung ADCs

We performed quantitative immunohistochemical (IHC) analysis of KL_{luc} mouse lung tumors following treatment (**Figure 4A**). Representative images and quantification of stains show phenformin + MLN0128 induced a 65% decrease in the Ki67 index (not significant) and a two fold increase in tumor cell death (significant) compared to vehicle treated KL_{luc} ADCs (**Figure 6A panel, 6B and 6C**). In contrast, phenformin alone or in combination with MLN0128 failed to suppress proliferation or induce apoptosis in K_{luc} lung tumors (**supplemental Figure S6A**). These results demonstrate that KL_{luc} lung tumors are selectively sensitive to phenformin and MLN0128 combination therapy.

We next performed quantitative IHC analysis of KL_{luc} and K_{luc} mouse lung tumors stained for P-S6 and HkII. Representative images and quantification of stains show MLN0128 alone or in combination with phenformin inhibited phosphorylation of S6 as compared to vehicle and phenformin treatment demonstrating that MLN0128 inhibited mTORC1 *in vivo* (**Figure 6A and 6D**). We next examined hexokinase II (HkII) expression in lung tumors from KL_{luc} and K_{luc} mice following treatment with phenformin, MLN0128, or combination therapy. HKII is a key enzyme for the intracellular retention and detection of 18F-FDG by PET and HKII enzymatic activity positively correlated with 18F-FDG uptake in human esophageal

tumors and xenografts of NSCLC(27),(28). We detected a significant reduction in HkII expression in MLN0128 and phenformin + MLN0128 treated lung tumors compared to vehicle in KL_{luc} mice. (**Figure 6A, 6E**) Interestingly, we observed only a modest reduction in P-S6 and HkII levels in MLN0128 and phenformin + MLN0128 treated K_{luc} lung tumors as represented by IHC staining (**Figures S6A, S6B**). This data agrees with previous work in which we observed low basal levels of P-S6 present in K_{luc} as compared to KL_{luc} lung tumors(7). The reduced efficacy of MLN0128 in K_{luc} mice may be explained by activation of the RAF/MEK/ERK pathway. We observed a nearly 2 fold increase phospho-Erk (P-Erk) staining (not significant) in MLN0128 and phenformin + MLN0128 treated lung tumors of K_{luc} mice (**Figure S6A, S6C**). P-Erk staining was not detectable in KL_{luc} lung tumors (data not shown), which agrees with previously published reports(29). These results show MLN0128 inhibited mTORC1 and HkII expression in $Kras^{G12D}$ driven lung tumors *in vivo*. The combination therapy cooperated to most effectively reduce tumor cell proliferation and viability in the KL_{luc} mice.

AKT activation is a common event in MLN0128 resistant KL_{luc} squamous lung tumors

To explain how KL_{luc} squamous lung tumors escaped MLN0128 single and combination therapy we investigated feedback signaling that may confer resistance. We examined the AKT pathway as previously published work on HER2 positive breast cancer cells identified a feedback loop that phosphorylated and activated AKT threonine 308 (P-AKT T308) in tumor cells following mTORC1/mTORC2 inhibition(30). We analyzed the AKT signaling pathway in p63 positive, surfactant protein c (SPC) negative SCCs lung tumor lysates (**Figure S7A**) from KL_{luc} mice that were treated with vehicle or MLN0128 for a duration of 8 weeks as described in Figure 4A. We show MLN0128 treatment reduced P-S6K and P-4E-BP1 levels in KL_{luc} SCC lung tumor lysates (represented by blue boxes) while inducing an increase in P-Akt T308 and its substrates phospho-Tuberous Sclerosis Complex 2 at threonine 1462 (P-Tsc2 T1462)(31) and phospho-Gsk α/β at serine 21 and 9 (P-Gskα/β S21/S9)(32) (represented by red boxes) (**Figure 7A**). IHC staining of therapy resistant KL_{luc} SCCs for P-Gskα/β (S21/S9) showed highest expression in MLN0128 and phenformin + MLN0128 treated tumors (**Figure 7B**). These results demonstrate that KL_{luc} SCC upregulate AKT signaling following mTORC1 inhibition.

We next performed an *in vitro* dose escalation in a $Kras^{G12D}$;*Lkb1*−/− (*KL*) MEFs to interrogate mTOR and AKT signaling at *in vivo* relevant doses of MLN0128. We showed that at increasing nanomolar doses, MLN0128 inhibited mTORC1 and concomitantly lead to the upregulation phospho-AKT-Thr308 (P-AKT T308) (**Figure S7C**). Comparison of P-S6K and P-4E-BP1 levels in immunoblots from KL_{luc} lung tumor lysates (**Figure 7A**) to those from KL MEFs (**Figure S7C**) showed comparable inhibition of mTORC1 and activation of P-Akt T308 by MLN0128 at a 20-100nM dose. These results agree with previously reported pharmacokinetic and pharmacodynamic analysis of MLN0128 in rodent models(17) and suggest that activation of P-AKT T308 following mTORC1 suppression may lead to MLN0128 resistance. We next combinatorially treated *LKB1*−/− RH2 SCC cells for 24 hours with low dose MLN0128 (20 and 100nM) and the AKT inhibitor MK2206 (1μM) and demonstrated MLN0128 + MK2206 completely abolished mTORC1 and AKT signaling as compared to no treatment (NT) or single therapy (**Figure 7C**). Combinatorial

treatment of a panel of lung SCC cells lines (n=7) with MLN0128 and MK2206 significantly reduced cell viability more effectively than either drug alone (**Figure 7D**). These results demonstrated an mTOR and AKT blockade as an effective strategy for targeting squamous cell lung carcinoma.

Discussion

In this study we found that co-mutations in *KRAS* and *LKB1* induce a tumor phenotype that is both sensitive to energetic stress and dependent upon mTORC1 signaling. We demonstrate that physiologically achievable doses of phenformin in combination with MLN0128 compound energetic stress in *KRAS/LKB1* mutant lung ADC resulting in restricted tumor growth and enhanced apoptosis in cell culture and in mice. Combinatorial use of phenformin and MLN0128 represent a clinically feasible therapeutic strategy to target this genetic subset of lung tumors. Oral delivery of phenformin at doses of phenformin originally defined for management of diabetes may represent a more practical approach to incorporate biguanides into cancer treatment regimens. For this reason we delivered phenformin ad lib in drinking water in combination with a once daily delivery of MLN0128 that showed no toxicity to animals and was well tolerated for the two-month treatment duration. Phase I dose escalation studies will be an important first step to begin testing phenformin as an anti-cancer agent in human lung cancer.

We demonstrate that MLN0128 robustly inhibited mTORC1 signaling *in vivo* and identified 4EBP1 as a key node downstream of mTORC1 that governs tumor cell survival expansion in *KRAS/LKB1* mutant NSCLC. It is possible that inhibition of 4E-BP1 and subsequent suppression of cap dependent translation may alter mitochondrial dynamics and cellular OXPHOS(33). MLN0128 and phenformin may also cooperate to disrupt the structural integrity of the mitochondria thus leading to caspase 3 mediated apoptosis. Alternatively, it is formally possible that reduced translation following mTOR inhibition may sensitize cells to phenformin through reduced expression of anti-apoptotic BCL2 proteins(34-36).

We have previously demonstrated mTORC1 is a key regulator of glycolysis in *LKB1*−/− cells through HIF1α and its target GLUT1(10). MLN0128 treatment downregulated the expression of the HIF1α and GLUT1 proteins and suppressed glucose metabolism, thus demonstrating that mTORC1 inhibition is an effective means to inhibit glycolysis in LKB1-deficient NSCLC. We show the combination of MLN0128 and phenformin lead to a severe reduction of cellular ATP and eventual metabolic crisis likely due to a dual inhibition both glycolysis and OXPHOS in LKB1-deficient tumors. Our data agree with a recent report that reduced breast tumor growth in *Lkb1*−/− NIC mice using the mTOR inhibitor AZ8055 in combination with an inhibitor of glycolysis, 2-deoxyglucose(7,37). 18FFDG PET guided pre-clinical studies on KL_{luc} and K_{luc} mice enabled us to examine glucose metabolism in lung tumors in real time as well as validate 18F-FDG as a biomarker for clinical evaluation of phenformin and MLN0128. In a recent study 18F-FDG PET was shown to be an accurate and dynamic biomarker to detect inhibition of glucose uptake following treatment with inhibitors of the mTORC1 and RAF/MEK/ERK pathway(30). Importantly, 18F-FDG PET and CT imaging of GEMMs in combination with IHC enabled us to identify therapy resistant SCC lung tumors that were metabolically responsive to mTORC1 inhibition. The

combined use of 18F-FDG PET and CT underscores the value of using multiple imaging modalities to evaluate both tumor size and tumor metabolism.

Phenformin dually inhibits mitochondrial complex I and induces the generation of reactive oxygen species (ROS)(38). In previous work we show that phenformin induced energetic stress as well as cytotoxic reactive oxygen species (ROS) resulting in apoptosis in *LKB1*−/− NSCLC cells(7). In this study we discovered that SCC were highly resistant to phenformin, which suggest squamous lung tumors are more resistant to phenformin induced mitochondrial insult and ROS than ADCs as was recently reported(39). Insensitivity of squamous lung tumors to phenformin may be explained by low mitochondria content that is fundamentally intrinsic to squamous cell biology(40). Furthermore, phenformin actively induces a cellular switch to glycolytic metabolism(41,42), which explains the expansion of FDG avid phenformin-resistant SCCs we observe in KL_{luc} mice (**Figures 4 and 5**). Phenformin mediated upregulation of glycolysis in SCC is expected to drive the pentose phosphate pathway (PPP) and fuel the production of NADPH leading to enhanced redox buffering and resistance to phenformin induced ROS. Additionally, SCC may buffer themselves against phenformin induced ROS through upregulation of cellular antioxidant pathways driven by the oxidative stress response as was recently shown in The Cancer Genome Atlas (TCGA) for lung squamous carcinoma(43).

The prevalence of therapy resistant SCC nodules may be explained by an adeno to squamous transdifferentiation (AST), which has been shown to occur in the *Kras/Lkb1* mouse lung cancer model(44). It is formally possible that phenformin and MLN0128 alone or in combination may drive ADCs to undergo a histological switch towards a squamous cell fate. This would be analogous to a tumor subtype switch observed *EGFR* mutant ADC that developed into small cell lung carcinomas (SCLC) following erlotinib treatment(45). Whether SCC tumors arose *de novo* or from AST, we conclude that the KL_{luc} SCC tumors would best be treated with MK2206 as a second line therapy or with an up front combination of MLN0128 and MK2206.

K_{luc} tumors were unresponsive to phenformin treatment consistent with our previous studies in which we demonstrated Lkb1 inactivation was required to mediate a response to phenformin(7). Unexpectedly, K_{luc} tumors showed only a modest response to MLN0128 or combination therapy. Failure of K_{luc} tumors to respond to MLN0128 may be explained by activation the RAF/MEF/ERK pathway is activated in K_{luc} lung tumors (**Figure S6A, S6C**). This suggests RAS driven lung tumors expressing functional LKB1 are predicted to respond better to MEK inhibitors (MEKi) as single therapy or in combination with mTOR inhibitors as was recently shown in RAS driven, *NF1* mutant neural sheath tumors co-treated with rapamycin and a MEKi(29,30,46).

The robust activation of AKT at threonine 308 in our KL_{luc} SCC lung tumors mirror a feedback loop first described in HER2 driven breast cancer(47), and suggest activation of AKT may be a conserved mechanism of acquired resistance to mTOR inhibition in SCC. As reported previously, chronic inhibition of mTORC1 leads to loss of feedback inhibition of PI3K signaling, resulting in the increased activity of PDK1 and increased P-AKT T308 phosphorylation levels(47). As MLN0128 resistant SCC tumors arose in mice treated with a

catalytic inhibitor of the mTOR kinase over 8 weeks, it also possible increased P-AKT T308 phosphorylation could occur as a result of increased expression levels of multiple receptor tyrosine kinases (RTK) as previously reported(48,49). Additionally, the persistent P-NDRG1 and P-AKT T473 signaling present in MLN0128 resistant SCC tumors (Figure 7A) may indicate mTORC2 activation contributed to therapy resistance. It will be necessary to interrogate the AKT-GSK signaling pathway and determine its role, if any towards conferring MLN0128 resistance. We show that using the AKT inhibitor MK2206 in combination with MLN0128 can suppress this signal transduction pathway *in vitro*, however, whether such combination would be efficient *in vivo* in a clinical setting remains to be determined.

The significant response of LKB1−/− SCC tumor cells to the combination of MLN0128 and MK2206 indicate an mTOR and AKT blockade may be an alternative therapeutic strategy for targeting KL_{luc} SCCs. Co-targeting mTORC1 and PI3K overcame rapamycin resistance in breast tumors with activating mutations in *PIK3CA*(50). Moreover, high AKT activation is frequently detected in human SCC and GEMMs of squamous lung cancer[41,](51,52). MK2206 is currently in clinical evaluation for NSCLC in the BATTLE2 biomarker integrated targeted therapy clinical trial (NCT01248247). Future biomarker driven clinical trials may seek to include MLN0128 in combination with MK2206 when targeting SCC. Biomarkers P-S6, P-4E-BP1 and P-GSKα/β (S21/9) could be readily utilized on formalin fixed paraffin embedded lung SCC biopsies to measure response or resistance to MLN0128 as single agents or in combination with MK2206. Our data suggest that *LKB1*−/− lung ADC may respond well to MLN0128 as a single therapy or in combination with phenformin, while SCC will likely respond best to an mTOR and AKT blockade. *LKB1* mutations either alone or in combination with *KRAS* occur frequently in NSCLC and constitute a large patient population that would likely benefit from the personalized therapies we have outlined(6,43).

Supplementary Material

Refer to Web version on PubMed Central for supplementary material.

Acknowledgments

We thank Dr. Reuben J. Shaw for critical review of the manuscript and feedback. We thank Darin Williams and Waldemar Ladno who performed PET and CT imaging on the mice and UCLA's Translational Pathology Core Laboratory for assistance with the Aperio and Definiens software. **Funding**: D.B.S. was supported by CTSI and KL2 Translational Science Award grant numbers KL2TR000122 and UL1TR000124 at the UCLA School of Medicine, the Addario Lung Cancer Research Foundation, the Dharma Master Jiantai Innovative Grant for Lung Cancer Research. D.B.S., T.C.W. and S.M.D. are supported by a D.O.D Lung Cancer Research Program Translational Research Partnership W81XWH-13-1-0459.

References

1. Lynch TJ, Bell DW, Sordella R, Gurubhagavatula S, Okimoto RA, Brannigan BW, et al. Activating mutations in the epidermal growth factor receptor underlying responsiveness of non-small-cell lung cancer to gefitinib. N Engl J Med. 2004; 350(21):2129–39. [PubMed: 15118073]
2. Kwak EL, Bang YJ, Camidge DR, Shaw AT, Solomon B, Maki RG, et al. Anaplastic lymphoma kinase inhibition in non-small-cell lung cancer. N Engl J Med. 2010; 363(18):1693–703. [PubMed: 20979469]

3. Perez-Moreno P, Brambilla E, Thomas R, Soria JC. Squamous Cell Carcinoma of the Lung: Molecular Subtypes and Therapeutic Opportunities. Clin Cancer Res. 2012; 18(9):2443–51. [PubMed: 22407829]
4. Sanchez-Cespedes M, Parrella P, Esteller M, Nomoto S, Trink B, Engles JM, et al. Inactivation of LKB1/STK11 is a common event in adenocarcinomas of the lung. Cancer Res. 2002; 62(13):3659–62. [PubMed: 12097271]
5. Wilkerson MD, Yin X, Walter V, Zhao N, Cabanski CR, Hayward MC, et al. Differential pathogenesis of lung adenocarcinoma subtypes involving sequence mutations, copy number, chromosomal instability, and methylation. PloS one. 2012; 7(5):e36530. [PubMed: 22590557]
6. Ding L, Getz G, Wheeler DA, Mardis ER, McLellan MD, Cibulskis K, et al. Somatic mutations affect key pathways in lung adenocarcinoma. Nature. 2008; 455(7216):1069–75. [PubMed: 18948947]
7. Shackelford DB, Abt E, Gerken L, Vasquez DS, Seki A, Leblanc M, et al. LKB1 inactivation dictates therapeutic response of non-small cell lung cancer to the metabolism drug phenformin. Cancer Cell. 2013; 23(2):143–58. [PubMed: 23352126]
8. Shaw RJ, Bardeesy N, Manning BD, Lopez L, Kosmatka M, DePinho RA, et al. The LKB1 tumor suppressor negatively regulates mTOR signaling. Cancer Cell. 2004; 6(1):91–9. [PubMed: 15261145]
9. Palaskas N, Larson SM, Schultz N, Komisopoulou E, Wong J, Rohle D, et al. 18F-fluorodeoxy glucose positron emission tomography marks MYC-overexpressing human basal-like breast cancers. Cancer Res. 2011; 71(15):5164–74. [PubMed: 21646475]
10. Shackelford DB, Vasquez DS, Corbeil J, Wu S, Leblanc M, Wu CL, et al. mTOR and HIF-1alpha-mediated tumor metabolism in an LKB1 mouse model of Peutz-Jeghers syndrome. Proc Natl Acad Sci U S A. 2009; 106(27):11137–42. [PubMed: 19541609]
11. Keith B, Johnson RS, Simon MC. HIF1alpha and HIF2alpha: sibling rivalry in hypoxic tumour growth and progression. Nat Rev Cancer. 2012; 12(1):9–22. [PubMed: 22169972]
12. Liang MC, Ma J, Chen L, Kozlowski P, Qin W, Li D, et al. TSC1 loss synergizes with KRAS activation in lung cancer development in the mouse and confers rapamycin sensitivity. Oncogene. 2010; 29(11):1588–97. [PubMed: 19966866]
13. Wander SA, Hennessy BT, Slingerland JM. Next-generation mTOR inhibitors in clinical oncology: how pathway complexity informs therapeutic strategy. The Journal of clinical investigation. 2011; 121(4):1231–41. [PubMed: 21490404]
14. Lou HZ, Weng XC, Pan HM, Pan Q, Sun P, Liu LL, et al. The novel mTORC1/2 dual inhibitor INK-128 suppresses survival and proliferation of primary and transformed human pancreatic cancer cells. Biochem Biophys Res Commun. 2014; 450(2):973–8. [PubMed: 24971544]
15. Slotkin E, Patwardhan PP, Deraje Vasudeva S, de Stanchina E, Tap WD, Schwartz GK. MLN0128, an ATP-Competitive mTOR Kinase Inhibitor, with Potent In vitro and In vivo Antitumor Activity as Potential Therapy for Bone and Soft-Tissue Sarcoma. Mol Cancer Ther. 2014
16. Zhang H, Dou J, Yu Y, Zhao Y, Fan Y, Cheng J, et al. mTOR ATP-competitive inhibitor INK128 inhibits neuroblastoma growth via blocking mTORC signaling. Apoptosis. 2014
17. Hsieh AC, Liu Y, Edlind MP, Ingolia NT, Janes MR, Sher A, et al. The translational landscape of mTOR signalling steers cancer initiation and metastasis. Nature. 2012; 485(7396):55–61. [PubMed: 22367541]
18. Pourdehnad M, Truitt ML, Siddiqi IN, Ducker GS, Shokat KM, Ruggero D. Myc and mTOR converge on a common node in protein synthesis control that confers synthetic lethality in Myc-driven cancers. Proc Natl Acad Sci U S A. 2013; 110(29):11988–93. [PubMed: 23803853]
19. Feldman ME, Apsel B, Uotila A, Loewith R, Knight ZA, Ruggero D, et al. Active-site inhibitors of mTOR target rapamycin-resistant outputs of mTORC1 and mTORC2. PLoS Biol. 2009; 7(2):e38. [PubMed: 19209957]
20. Thoreen CC, Kang SA, Chang JW, Liu Q, Zhang J, Gao Y, et al. An ATP-competitive mTOR inhibitor reveals rapamycin-insensitive functions of mTORC1. J Biol Chem. 2009

21. Dowling RJ, Topisirovic I, Alain T, Bidinosti M, Fonseca BD, Petroulakis E, et al. mTORC1-mediated cell proliferation, but not cell growth, controlled by the 4E-BPs. Science. 2010; 328(5982):1172–6. [PubMed: 20508131]
22. Thoreen CC, Chantranupong L, Keys HR, Wang T, Gray NS, Sabatini DM. A unifying model for mTORC1-mediated regulation of mRNA translation. Nature. 2012; 485(7396):109–13. [PubMed: 22552098]
23. She QB, Halilovic E, Ye Q, Zhen W, Shirasawa S, Sasazuki T, et al. 4E-BP1 is a key effector of the oncogenic activation of the AKT and ERK signaling pathways that integrates their function in tumors. Cancer Cell. 2010; 18(1):39–51. [PubMed: 20609351]
24. Faubert B, Vincent EE, Griss T, Samborska B, Izreig S, Svensson RU, et al. Loss of the tumor suppressor LKB1 promotes metabolic reprogramming of cancer cells via HIF-1alpha. Proc Natl Acad Sci U S A. 2014; 111(7):2554–9. [PubMed: 24550282]
25. Gwinn DM, Shackelford DB, Egan DF, Mihaylova MM, Mery A, Vasquez DS, et al. AMPK phosphorylation of raptor mediates a metabolic checkpoint. Mol Cell. 2008; 30(2):214–26. [PubMed: 18439900]
26. Ji H, Ramsey MR, Hayes DN, Fan C, McNamara K, Kozlowski P, et al. LKB1 modulates lung cancer differentiation and metastasis. Nature. 2007; 448(7155):807–10. [PubMed: 17676035]
27. Fukunaga T, Enomoto K, Okazumi S, Kikuchi T, Yamamoto H, Koide Y, et al. [Analysis of glucose metabolism in patients with esophageal cancer by PET: estimation of hexokinase activity in the tumor and usefulness for clinical assessment using 18F-fluorodeoxyglucose]. Nihon Geka Gakkai Zasshi. 1994; 95(5):317–25. [PubMed: 8007937]
28. Su H, Bodenstein C, Dumont RA, Seimbille Y, Dubinett S, Phelps ME, et al. Monitoring tumor glucose utilization by positron emission tomography for the prediction of treatment response to epidermal growth factor receptor kinase inhibitors. Clin Cancer Res. 2006; 12(19):5659–67. [PubMed: 17020967]
29. Chen Z, Cheng K, Walton Z, Wang Y, Ebi H, Shimamura T, et al. A murine lung cancer co-clinical trial identifies genetic modifiers of therapeutic response. Nature. 2012; 483(7391):613–7. [PubMed: 22425996]
30. Malone CF, Fromm JA, Maertens O, DeRaedt T, Ingraham R, Cichowski K. Defining key signaling nodes and therapeutic biomarkers in NF1-mutant cancers. Cancer Discov. 2014; 4(9): 1062–73. [PubMed: 24913553]
31. Manning BD, Tee AR, Logsdon MN, Blenis J, Cantley LC. Identification of the tuberous sclerosis complex-2 tumor suppressor gene product tuberin as a target of the phosphoinositide 3-kinase/akt pathway. Mol Cell. 2002; 10(1):151–62. [PubMed: 12150915]
32. Cross DA, Alessi DR, Cohen P, Andjelkovich M, Hemmings BA. Inhibition of glycogen synthase kinase-3 by insulin mediated by protein kinase B. Nature. 1995; 378(6559):785–9. [PubMed: 8524413]
33. Morita M, Gravel SP, Chenard V, Sikstrom K, Zheng L, Alain T, et al. mTORC1 controls mitochondrial activity and biogenesis through 4E-BP-dependent translational regulation. Cell Metab. 2013; 18(5):698–711. [PubMed: 24206664]
34. Faber AC, Coffee EM, Costa C, Dastur A, Ebi H, Hata AN, et al. mTOR inhibition specifically sensitizes colorectal cancers with KRAS or BRAF mutations to BCL-2/BCL-XL inhibition by suppressing MCL-1. Cancer Discov. 2014; 4(1):42–52. [PubMed: 24163374]
35. Preuss E, Hugle M, Reimann R, Schlecht M, Fulda S. Pan-mammalian target of rapamycin (mTOR) inhibitor AZD8055 primes rhabdomyosarcoma cells for ABT-737-induced apoptosis by down-regulating Mcl-1 protein. J Biol Chem. 2013; 288(49):35287–96. [PubMed: 24133218]
36. Wei G, Twomey D, Lamb J, Schlis K, Agarwal J, Stam RW, et al. Gene expression-based chemical genomics identifies rapamycin as a modulator of MCL1 and glucocorticoid resistance. Cancer Cell. 2006; 10(4):331–42. [PubMed: 17010674]
37. Andrade-Vieira R, Goguen D, Bentley HA, Bowen CV, Marignani PA. Pre-clinical study of drug combinations that reduce breast cancer burden due to aberrant mTOR and metabolism promoted by LKB1 loss. Oncotarget. 2014
38. Bridges HR, Jones AJ, Pollak MN, Hirst J. Effects of metformin and other biguanides on oxidative phosphorylation in mitochondria. Biochem J. 2014; 462(3):475–87. [PubMed: 25017630]

39. Li F, Han X, Li F, Wang R, Wang H, Gao Y, et al. LKB1 Inactivation Elicits a Redox Imbalance to Modulate Non-small Cell Lung Cancer Plasticity and Therapeutic Response. Cancer Cell. 2015; 27(5):698–711. [PubMed: 25936644]
40. Borland R, Webber AJ. An electron microscope study of squamous cell carcinoma in merino sheep associated with keratin-filled cysts of the skin. Cancer Res. 1966; 26(1):172–82. [PubMed: 5948105]
41. Vincent EE, Coelho PP, Blagih J, Griss T, Viollet B, Jones RG. Differential effects of AMPK agonists on cell growth and metabolism. Oncogene. 2014
42. Dykens JA, Jamieson J, Marroquin L, Nadanaciva S, Billis PA, Will Y. Biguanide-induced mitochondrial dysfunction yields increased lactate production and cytotoxicity of aerobically-poised HepG2 cells and human hepatocytes in vitro. Toxicol Appl Pharmacol. 2008; 233(2):203–10. [PubMed: 18817800]
43. Hammerman PS, Lawrence MS, Voet D, Jing R, Cibulskis K, Sivachenko A, et al. Comprehensive genomic characterization of squamous cell lung cancers. Nature. 2012
44. Han X, Li F, Fang Z, Gao Y, Fang R, Yao S, et al. Transdifferentiation of lung adenocarcinoma in mice with Lkb1 deficiency to squamous cell carcinoma. Nat Commun. 2014; 5:3261. [PubMed: 24531128]
45. Sequist LV, Waltman BA, Dias-Santagata D, Digumarthy S, Turke AB, Fidias P, et al. Genotypic and histological evolution of lung cancers acquiring resistance to EGFR inhibitors. Sci Transl Med. 2011; 3(75):75ra26.
46. Engelman JA, Chen L, Tan X, Crosby K, Guimaraes AR, Upadhyay R, et al. Effective use of PI3K and MEK inhibitors to treat mutant Kras G12D and PIK3CA H1047R murine lung cancers. Nat Med. 2008; 14(12):1351–6. [PubMed: 19029981]
47. Rodrik-Outmezguine VS, Chandarlapaty S, Pagano NC, Poulikakos PI, Scaltriti M, Moskatel E, et al. mTOR kinase inhibition causes feedback-dependent biphasic regulation of AKT signaling. Cancer Discov. 2011; 1(3):248–59. [PubMed: 22140653]
48. O'Reilly KE, Rojo F, She QB, Solit D, Mills GB, Smith D, et al. mTOR inhibition induces upstream receptor tyrosine kinase signaling and activates Akt. Cancer Res. 2006; 66(3):1500–8. [PubMed: 16452206]
49. Rozengurt E, Soares HP, Sinnet-Smith J. Suppression of feedback loops mediated by PI3K/mTOR induces multiple overactivation of compensatory pathways: an unintended consequence leading to drug resistance. Mol Cancer Ther. 2014; 13(11):2477–88. [PubMed: 25323681]
50. Elkabets M, Vora S, Juric D, Morse N, Mino-Kenudson M, Muranen T, et al. mTORC1 inhibition is required for sensitivity to PI3K p110alpha inhibitors in PIK3CA-mutant breast cancer. Sci Transl Med. 2013; 5(196):196ra99.
51. Xu C, Fillmore CM, Koyama S, Wu H, Zhao Y, Chen Z, et al. Loss of Lkb1 and Pten leads to lung squamous cell carcinoma with elevated PD-L1 expression. Cancer Cell. 2014; 25(5):590–604. [PubMed: 24794706]
52. Mukhopadhyay A, Berrett KC, Kc U, Clair PM, Pop SM, Carr SR, et al. Sox2 cooperates with Lkb1 loss in a mouse model of squamous cell lung cancer. Cell Rep. 2014; 8(1):40–9. [PubMed: 24953650]

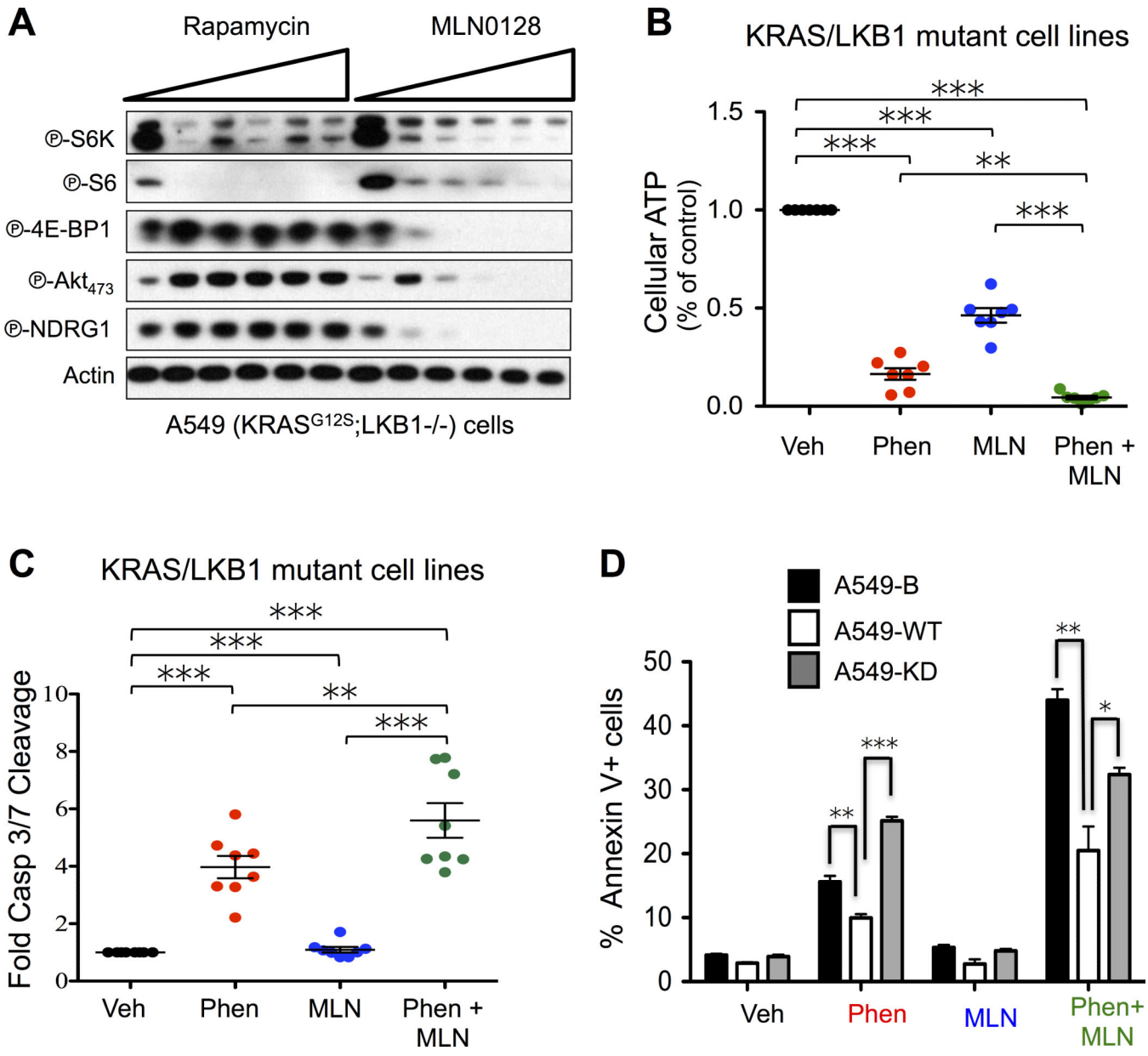

Figure 1. Phenformin and the mTOR kinase inhibitor MLN0128 compound energy stress to induce apoptosis in *KRAS/LKB1* mutant NSCLC cells

(A) A549 NSCLC cells were treated with increasing doses of MLN0128 or rapamycin. Immunoblots were probed with the indicated antibodies. (B and C) Cellular ATP measurement using cell titer and caspase 3/7 glo assays. *LKB1* and *KRAS/LKB1* mutant tumor lines (A549, H157, H460, A427, H1568, H23, H838, and RH2) were treated with DMSO (NT), phenformin (2mM), MLN0128 (2μM) or phenformin + MLN0128 for 24 hours. (D) Flow cytometry analysis of A549 cells expressing pBABE vector (B), wildtype LKB1 (WT) or kinase dead LKB1 (KD) that were treated with DMSO (NT), phenformin (2mM), MLN0128 (2μM) or phenformin + MLN0128 for 24 hours. Annexin V staining of A549-B, WT and KD cells following 24 hours of treatment. Statistical significance (p-values: * < 0.05; ** < 0.01; *** < 0.001) calculated using a non-parametric one-way

ANOVA (Tukey test). The data are represented as the mean ± SEM. Error bars represent the ± S.E.M.

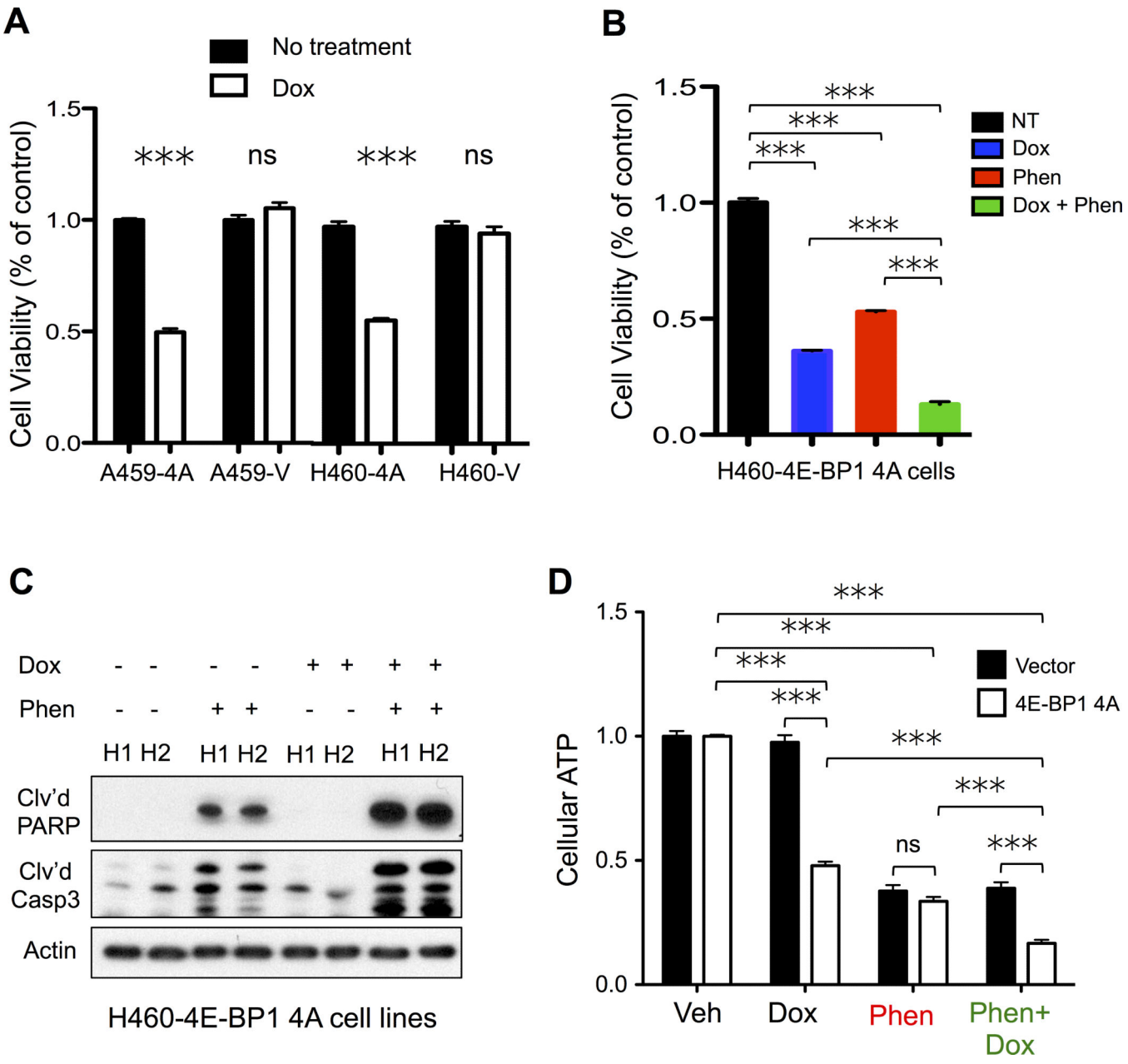

Figure 2. 4E-BP1 is a regulator of cell survival and energetics in *KRAS/LKB1* mutant NSCLC tumor cells

(A) Trypan blue cell viability assay of A549 and H460 cells expressing 4E-BP1 4Ala (A549-4A; H460-4A) or vector (A549-V; H460-V) that were either not treated (NT) or treated with 1μg/ml doxycycline (Dox) for 3 days. (B-D) H460-4A cells were either untreated (NT) or treated with 1μg/ml doxycycline for two days (Dox). NT and Dox treated cells were then treated with 2mM phenformin for 24 hours (Phen) and (Dox+Phen). Cell viability, cell lysates and cellular ATP were analyzed. (B) Cell viability by trypan blue staining of NT, Dox, Phen and Dox+Phen H460-4A cells. (C) Immunoblots of H460-4A lysates probed with antibodies recognizing cleaved PARP (Clv'd PARP), cleaved caspase 3 (Clv'd Casp3) and actin. (D) Cellular ATP measurement by cell titer glo in H460-4A cells.

Statistical significance (p-values: * < 0.05; ** < 0.01; *** < 0.001) calculated using a non-parametric one-way ANOVA (Tukey test). The data are represented as the mean ± SEM. Error bars represent the ± S.E.M.

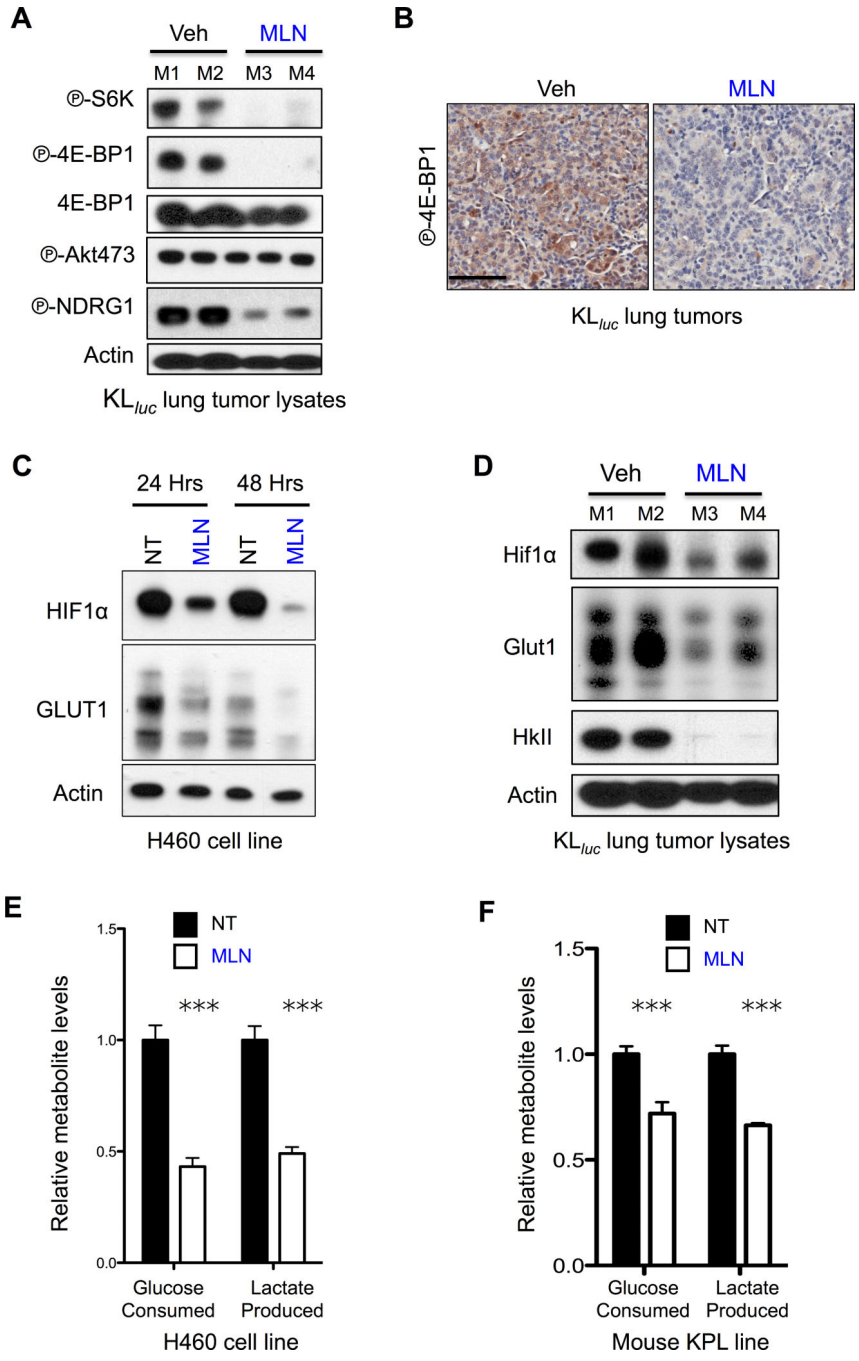

Figure 3. MLN0128 inhibited glucose metabolism in *KRAS/LKB1* mutant NSCLC *in vitro* and *in vivo*

(A) Lung tumor lysates from tumors isolated from KL_{luc} mice (M1, M2, M3 or M4) that were treated with vehicle (Veh) or MLN0128 (MLN) for five days were probed with indicated antibodies. (B) IHC staining of P-4E-BP1 in KL_{luc} lung tumors following five days MLN0128 treatment. Scale bars (black) = 50μM. (C) H460 cell line was treated with vehicle (NT) or 2μM MLN128 (MLN) for 24hr or 48hr. Lysates were probed with indicated antibodies. (D) Lung tumor lysates from tumors isolated from KL_{luc} mice (M1, M2, M3 or M4) that were treated with vehicle (Veh) or MLN0128 (MLN) for 5 days were probed with

indicated antibodies. (E and F) Relative levels of glucose consumption and lactate production in H460 cells (E) or lung tumor cell line derived from a $Kras^{G12D};p53^{-/-};Lkb1^{-/-}$ (KPL) mouse that were treated with vehicle (NT) or 2μM MLN0128 (MLN) for 24 hours. Statistical significance (p-values: * < 0.05; ** < 0.01; *** < 0.001;) calculated using a non-parametric one-way ANOVA (Tukey test). The data are represented as the mean ± SEM. Error bars represent the ± S.E.M.

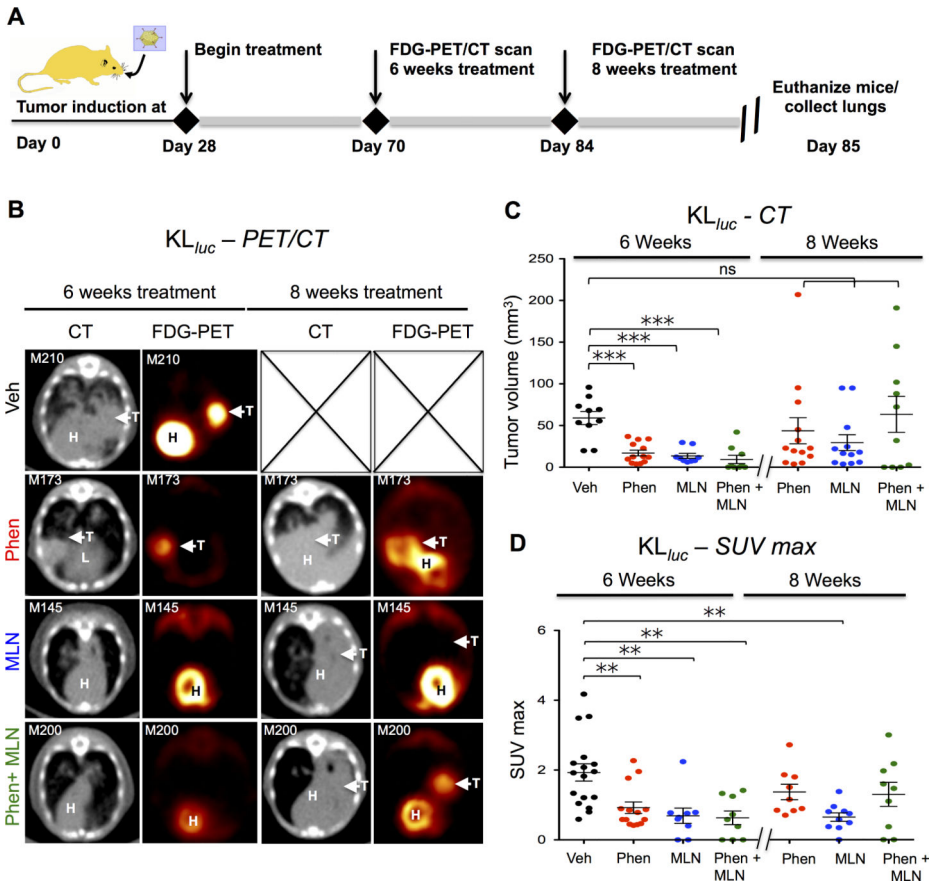

Figure 4. FDG-PET guided treatment of KL$_{luc}$ GEMMs revealed MLN0128 as a single agent or in combination with phenformin induced a significant metabolic and therapeutic response in lung tumors

(A) A schematic showing the treatment regimen for KL$_{luc}$ mice. Mice were fed phenformin ad lib in drinking water (1.8mg/mL) and given an i.p. injection of vehicle (PEG/NMP) or MLN128 1.0mg/kg q.d. (B) 18F-FDG-PET and CT images of KL$_{luc}$ mice at 6 weeks and 8 weeks post treatment with vehicle, phenformin, MLN0128 or phenformin + MLN0128. (C) Quantitative measure of tumor volume by CT of KL$_{luc}$ mice at 6 and 8 weeks post treatment. **(**D) Quantitative measure of SUVmax by 18F-FDG PET of KL$_{luc}$ mice at 6 and 8 weeks post treatment. Statistical significance (p-values: * < 0.05; ** < 0.01; *** < 0.001) calculated using a non-parametric one-way ANOVA (Tukey test). The data are represented as the mean ± SEM. Error bars represent the ± S.E.M.

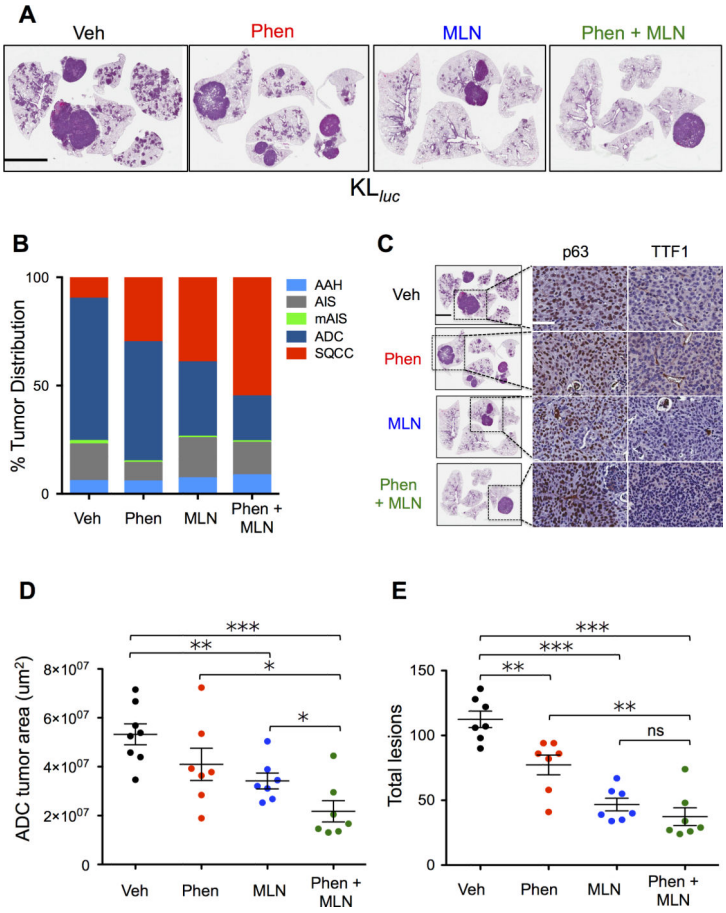

Figure 5. Phenformin and MLN0128 therapy induced a differential therapeutic response between KL$_{luc}$ lung adenocarcinomas and squamous cell carcinomas

(A) Representative H&E images of KL$_{luc}$ whole lungs following 8 weeks treatment with vehicle, phenformin, MLN0128 or phenformin + MLN0128 combination therapy (as described in Figure 4A). Scale bars (black) = 4mm. (B) Distribution of KL$_{luc}$ lung tumor subtypes: atypical adenomatous hyperplasia (AAH), adenocarcinoma in situ (AIS), mucinous adenocarcinoma in situ (mAIS), adenocarcinoma (ADC), squamous cell carcinoma SCC following treatment. (C) IHC staining of therapy resistant lung tumors with antibodies against p63 and TTF1. Scale bars (white) = 50μM. (D) Quantitative histology analysis of lung ADC tumor area from H&E stained whole lung sections of KL$_{luc}$ mice using morphometric analysis software. (E) Total lesion counts in whole lung sections of KL$_{luc}$ mice. Statistical significance (p-values: * < 0.05; ** < 0.01; *** < 0.001;) calculated using a non-parametric one-way ANOVA (Tukey test). The data are represented as the mean ± SEM. Error bars represent the ± S.E.M.

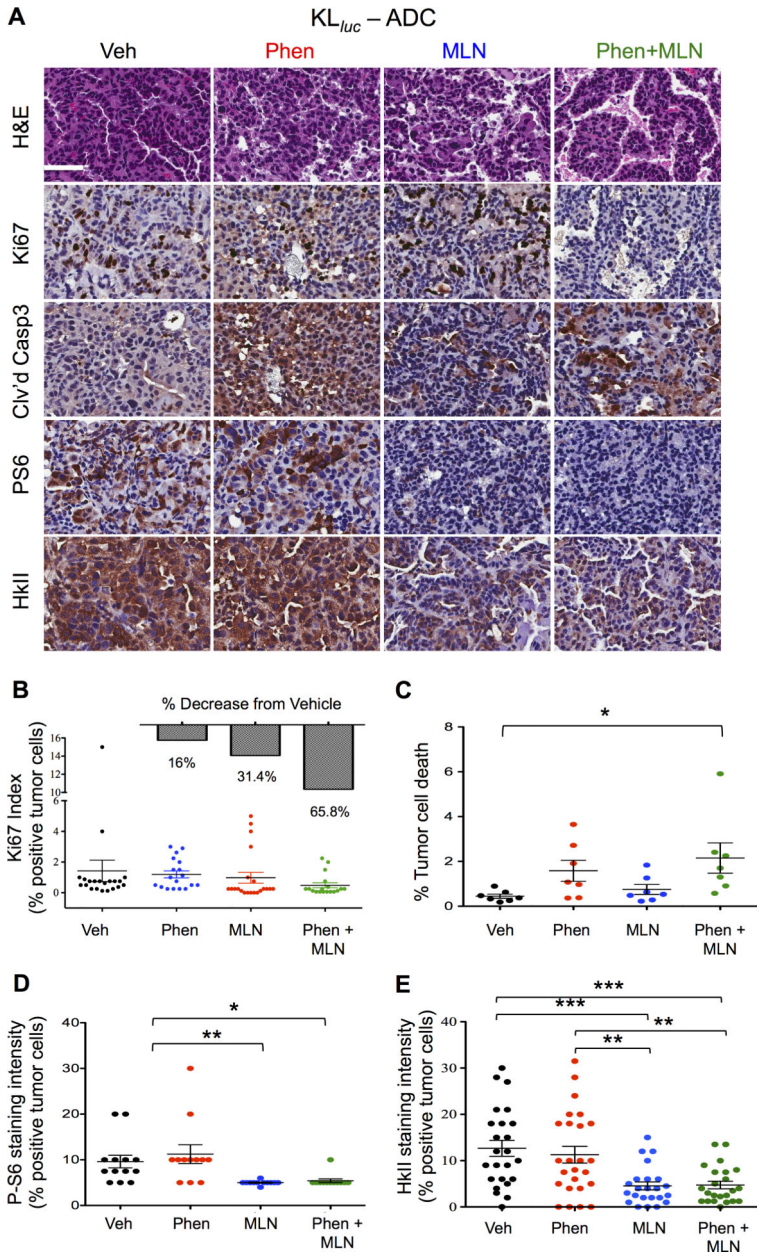

Figure 6. Phenformin + MLN0128 combination therapy inhibit tumor cell proliferation and induce apoptosis in KL$_{luc}$ lung ADCs

(A) Immunohistochemical analysis of lung ADCs from KL$_{luc}$following 8 weeks of treatment. Whole lung sections were stained with H&E or the indicated antibodies: Ki67, cleaved caspase 3 (Clv'd Casp3), P-S6 or HkII. Scale bars (white) = 50μM. (B-E) Quantitative IHC analysis of whole lung sections from KL$_{luc}$ mice stained Ki67, cleaved caspase 3, PS6 and HkII. Statistical significance (p-values: * < 0.05; ** < 0.01; *** < 0.001) calculated using a non-parametric one-way ANOVA (Tukey test). The data are represented as the mean ± SEM. Error bars represent the ± S.E.M.

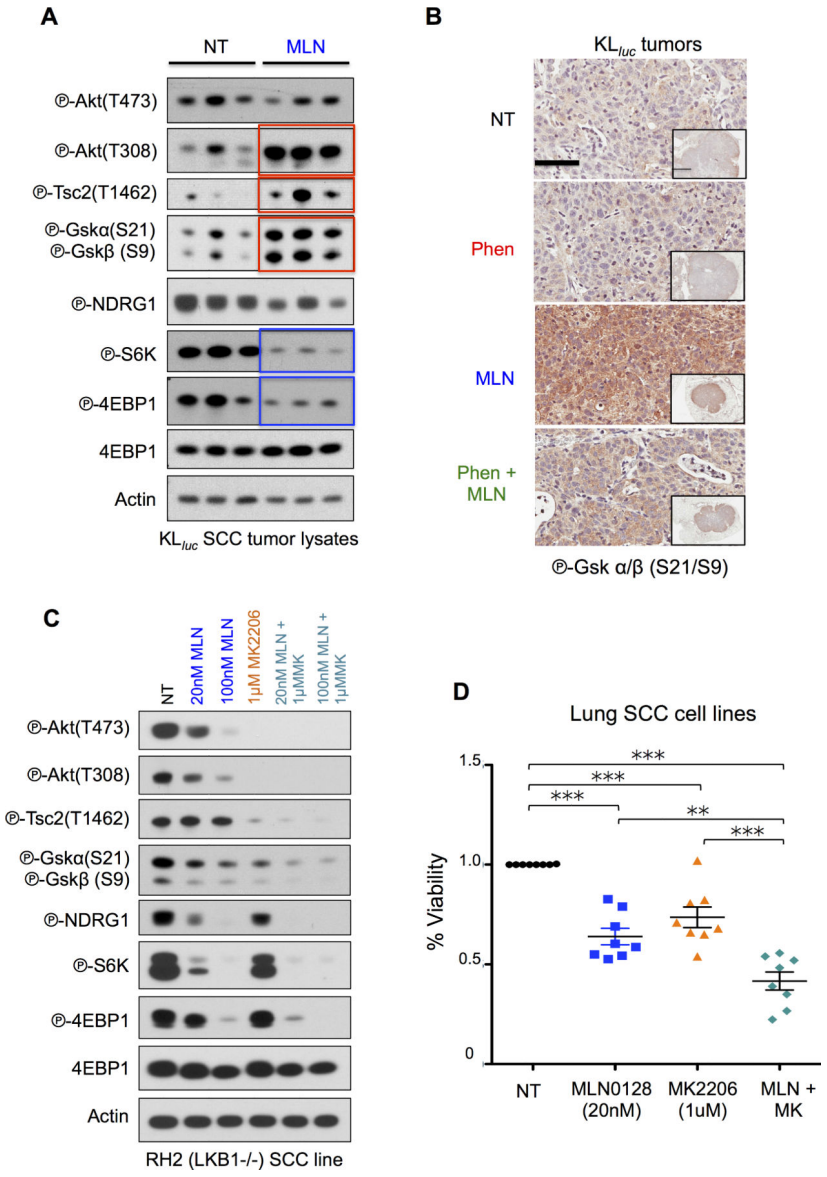

Figure 7. Co-targeting SCC with MLN0128 and MK2206

(A) Analysis of lung tumor lysates from KL_{luc} SCC following 8 weeks of MLN0128 treatment. Immunoblots were stained with the indicated antibodies. (B) Immunoblots from whole cell lysates from RH2 cells treated with DMSO, MLN0128 (20nM and 100nM), MK2206 (1μM), 20nM MLN0128 + 1μM MK2206 and 100nM MLN0128 + 1μM MK2206 for 24hours. Immunoblots were stained with the indicated antibodies. (C) Representative immunohistochemistry images from therapy resistant SCC tumors stained with phospho-GSKα/β (Ser21/9) antibody. Scale bars (black) = 50 μM and inset = 2mm. (D) Cell viability measured by trypan blue staining of SCC cell lines (RH2, H157, H226, H460, H520, H596, H1703, and SW900) treated with DMSO, low dose MLN0128 (20nM), MK2206 (1μM) or MLN0128 (20nM) + MK2206 (1μM) for 3 days. Statistical significance (p-values: * < 0.05;

** < 0.01; *** < 0.001;) calculated using a non-parametric one-way ANOVA (Tukey test). The data are represented as the mean ± SEM. Error bars represent the ± S.E.M.